Electronic Supplementary Material (ESI) for Journal of Materials Chemistry A.

Supporting Information

Decoding Crystal Engineering of Graphite-Like Energetic Materials: From Theoretical Prediction to Experimental Verification

Siwei Song, Yi Wang *, Kangcai Wang, Fang Chen and Qinghua Zhang*

Table of Contents

`

Figure S1. The illustration of coplanar configuration searching (CCS) and parameter settings test

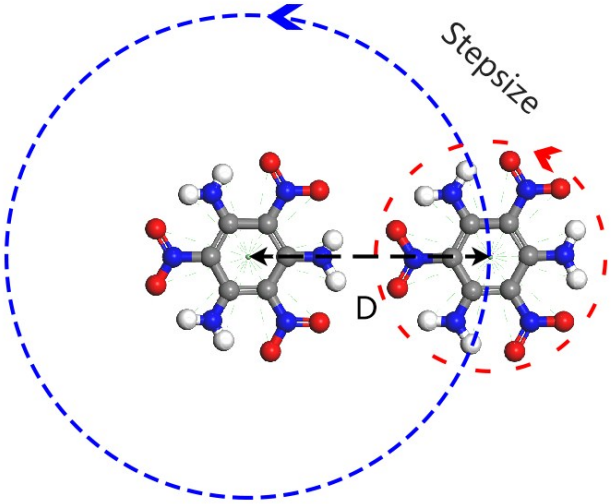

To confirm all the possible coplanar configuration dimers from the view of energy, a coplanar configuration searching (CCS) was implemented.

The optimization were performed with Dmol3 program. Setting parameters were as follows: the theory level was GGA/PBE, and DNP basis set was adopted. Dispersion correction was also considered using Grimme's method.[1] The convergence tolerance for energy, maximum force and maximum displacement were set to 1.0e-5 Ha, 0.002Ha/Å and 0.005Å, respectively.

To conserve time and reduce operating error, all the CCS calculation procedures were accomplished by a home-made perl script based on Dmol3 module in Materials studio 8.0.

Figure S2. Convergence tolerance test of coplanar configuration searching (CCS)

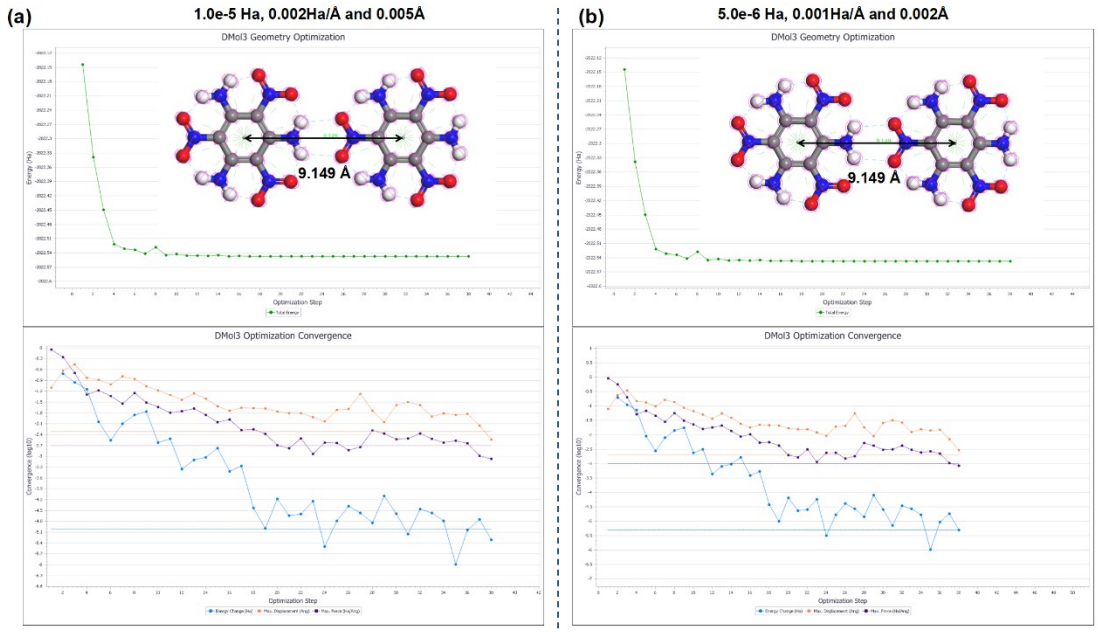

To ensure the sensitivity and reliability of the calculation results, we also improved the convergence tolerance to 5.0e-6 Ha, 0.001Ha/Å and 0.002Å and the comparison

test was launched on a TATNBZ dimer. When the optimization converged, the calculated single point energy (-2022.5474783Ha) and optimized geometries for former (1.0e-5 Ha, 0.002Ha/Å and 0.005Å) and later (5.0e-6 Ha, 0.001Ha/Å and 0.002Å) tolerance are totally identical as shown in Figure S2. Thus, we think the chosen tolerance (1.0e-5 Ha, 0.002Ha/Å and 0.005Å) are reasonable and adequate for our cases.

Figure S3. Molecular geometries of 92 molecules after two steps screening.

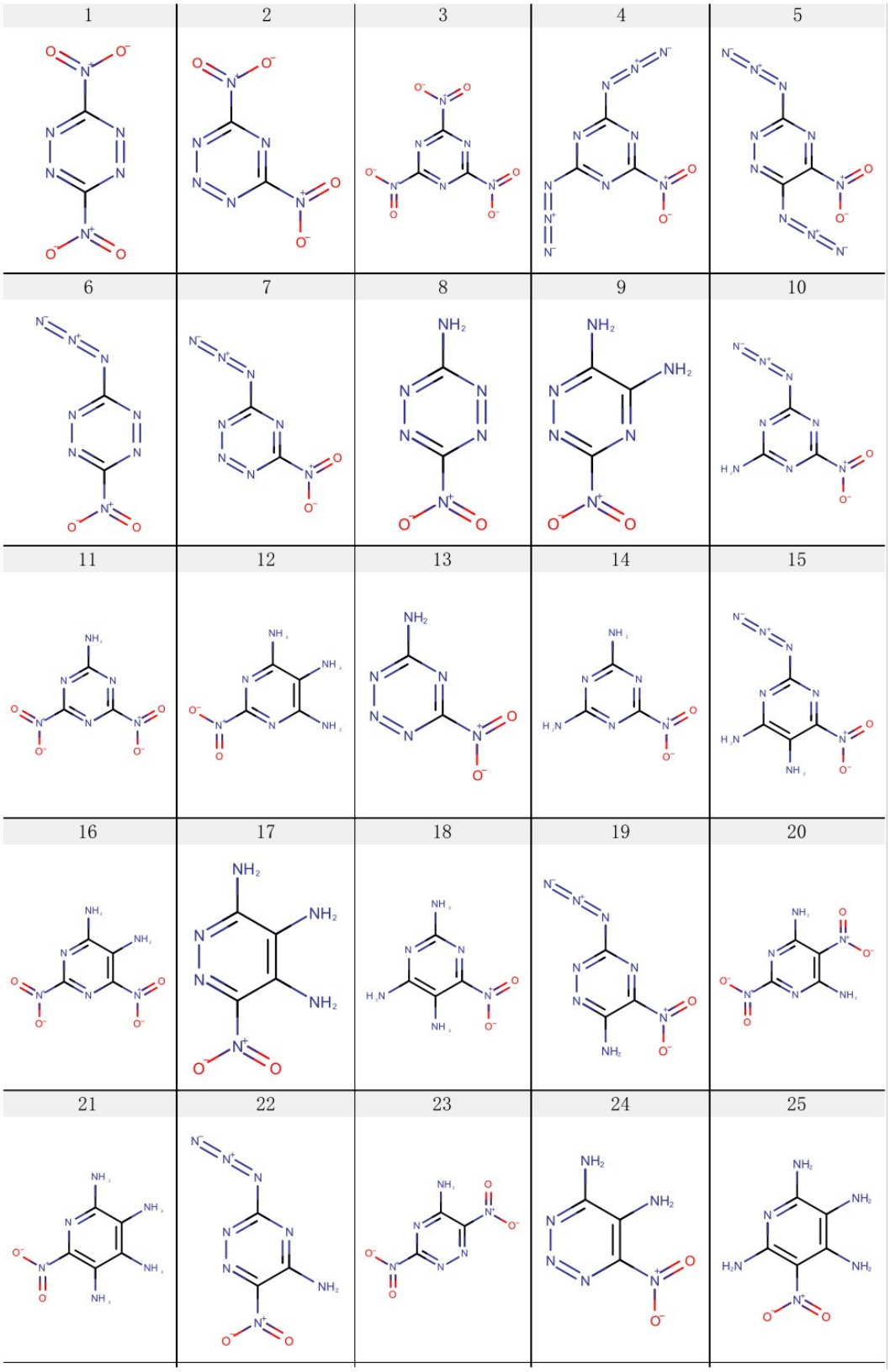

26	27	28	29	30
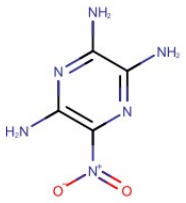	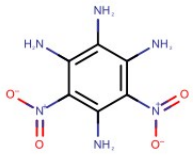	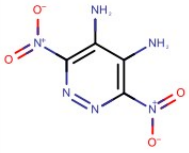	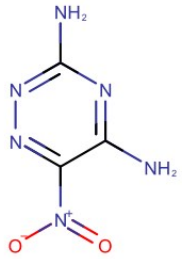	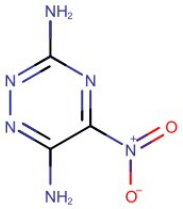
31	32	33	34	35
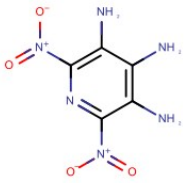	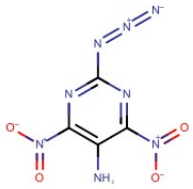	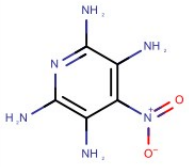	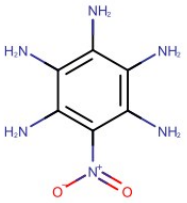	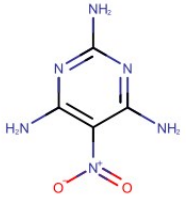
36	37	38	39	40
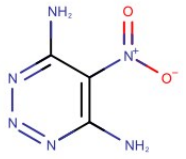	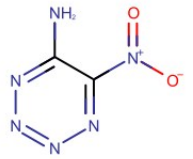	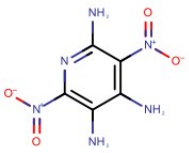	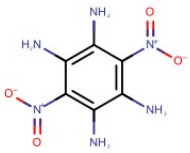	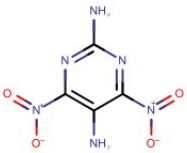
41	42	43	44	45
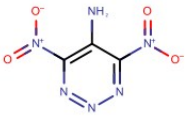	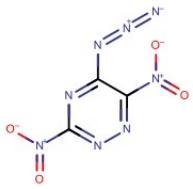	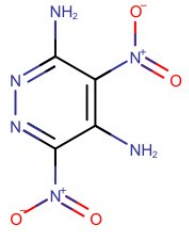	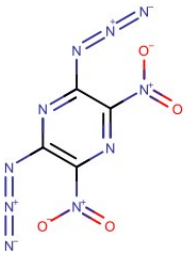	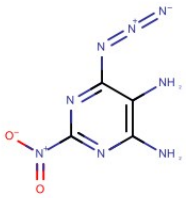
46	47	48	49	50
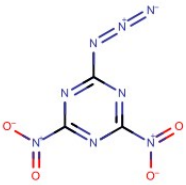	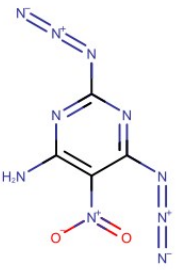	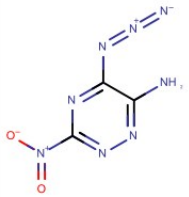	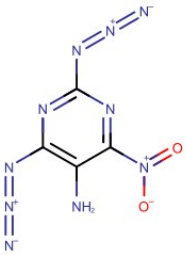	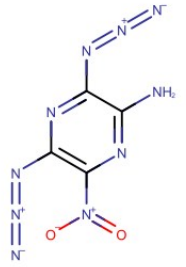

51	52	53	54	55
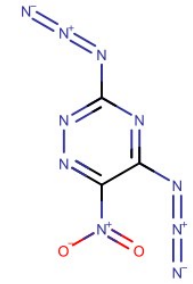	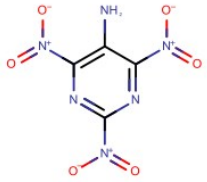	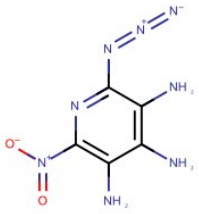	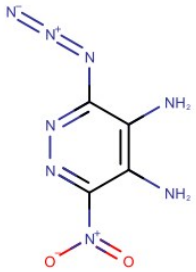	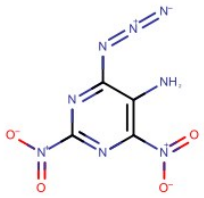
56	57	58	59	60
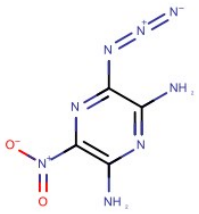	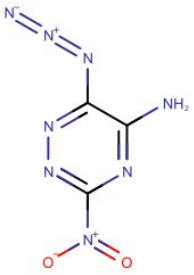	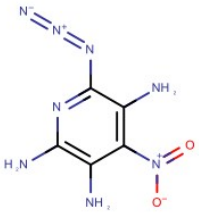	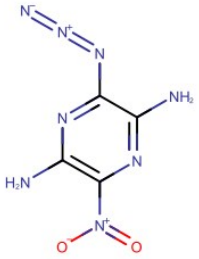	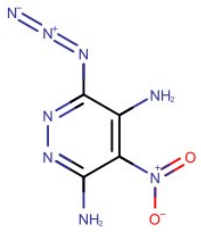
61	62	63	64	65
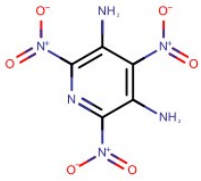	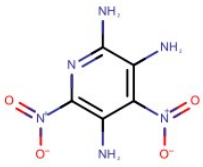	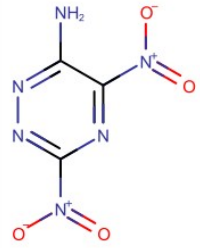	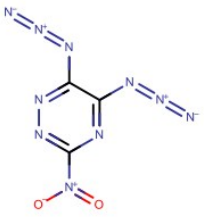	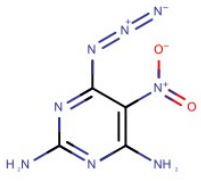
66	67	68	69	70
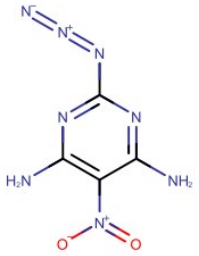	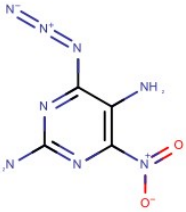	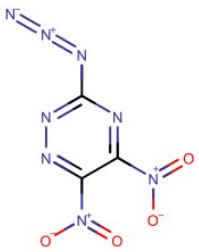	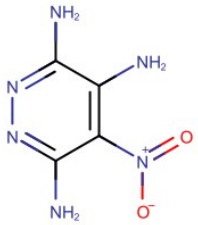	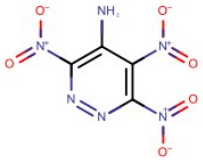
71	72	73	74	75
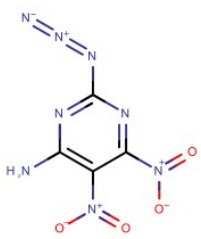	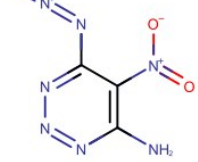	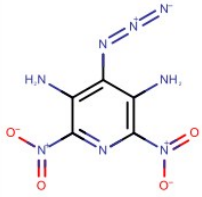	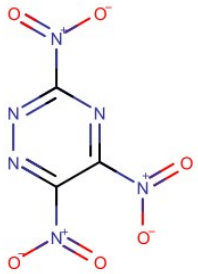	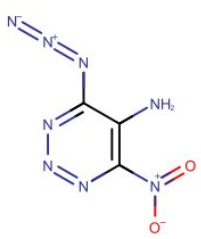

76	77	78	79	80
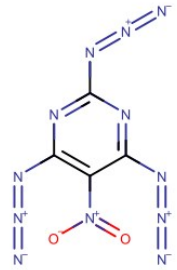	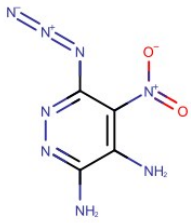	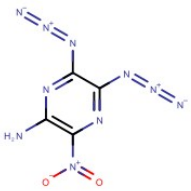	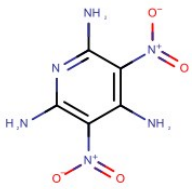	
81	82	83	84	85
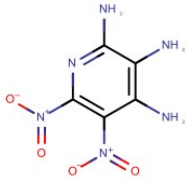	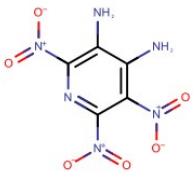	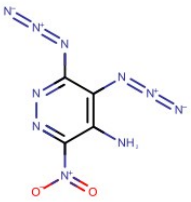	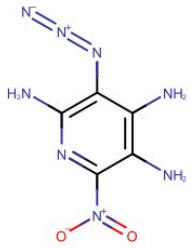	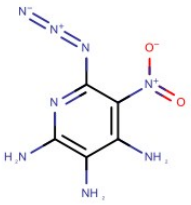
86	87	88	89	90
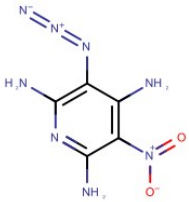	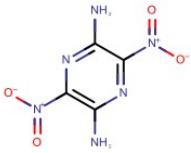	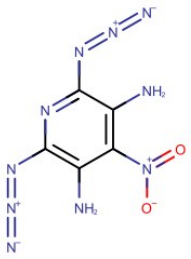	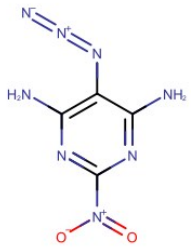	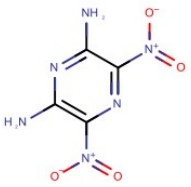
91	92			
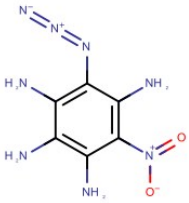	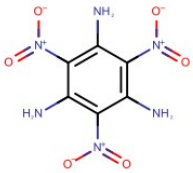			

Figure S4. Screening criteria for molecular density and PBF

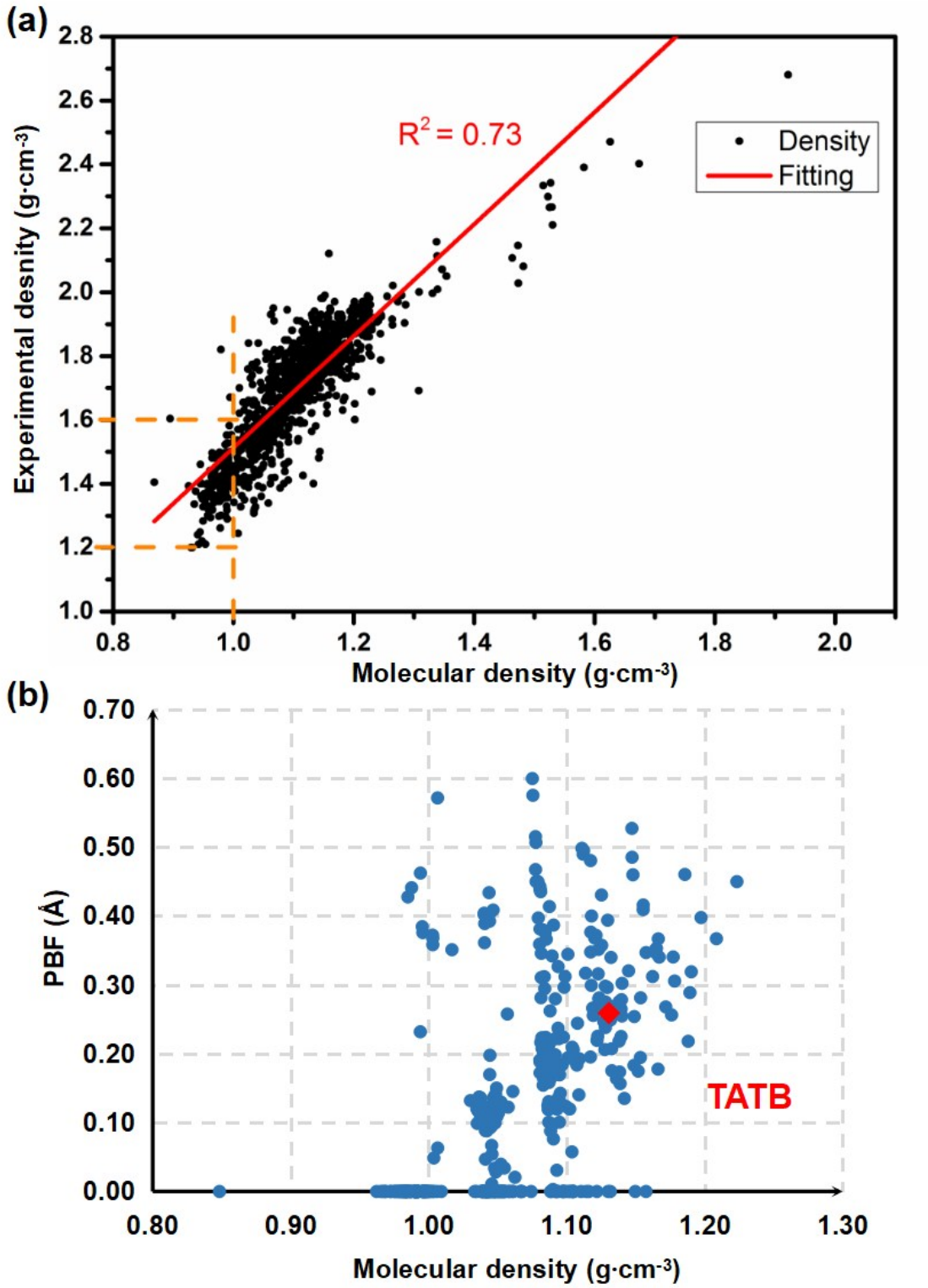

It is well known that the accurate crystal density prediction of energetic molecules is very challenging at present. But the theoretically molecular densities of energetic molecules are relatively facilitated to be obtained with a simple calculation of theoretical molar mass divided by theoretical molecular molar volume. Regretfully, the theoretically molecular densities usually exhibit a large deviation to the experimental ones. Based on data correlation analysis of more than one thousand energetic molecules between experimental crystal densities and theoretically molecular densities, we found that the experimental crystal densities actually have a close relationship to the theoretically molecular densities (Figure S4a). In general, high theoretically molecular densities imply high experimental crystal densities. As shown in Figure S4a, for the molecules with a molecular density lower than 1.00 $g \cdot cm^{-3}$, the experimental densities are lower than 1.6 $g \cdot cm^{-3}$ in most cases. Considering the positive correlation between detonation properties and density, we think the molecular density that in the first step screening can be set to 1.00 $g \cdot cm^{-3}$ to guarantee the energy level of screened molecules.

In determining the PBF threshold, we use TATB as a norm. TATB is a classical energetic material with graphite-like structure and planar geometry. We think molecules with more flat geometries than TATB (PBF values lower than that of TATB) are more favorable to assembly a flat molecular plane form the topology view. In addition, in the generated 426 molecules the PBF of TATB was in the middle position as shown in Figure S4b. We think it is appropriate to use the PBF value of TATB as a standard, neither too strict nor too loose. The PBF value for TATB after geometry optimization by molecular mechanics and DFT method are 0.26 Å and 0.21 Å, respectively. Considering the relatively low accuracy of molecular mechanics method, we relax the PBF restriction in the first screening step from 0.26 Å to 0.30Å.

Figure S5. Theoretical deduction of P2NAADD, P2NNAAD, P3NAAD-5 and P3NNAD-1 on graphite-like crystal structure by CCS and pcp-PIA methods

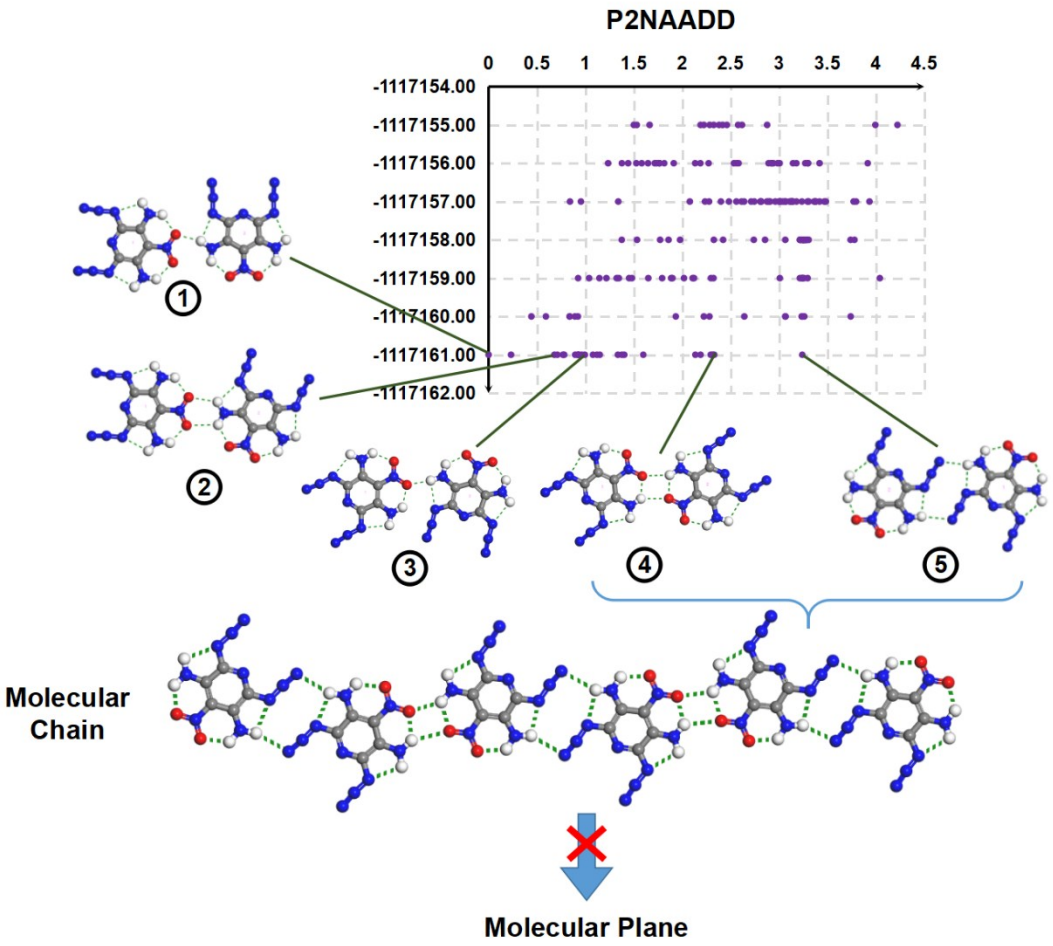

The CCS results of P2NAADD demonstrate that several dimers like 1, 2, 3, 4, 5 hold a plannar geometry and meanwhile the lowest energy. Starting with dimer 4 and 5, a molecular chain can be constructed. However, the "chain" can not be extended into a "plane" through the reasonable unsaturated hydrogen bond according to the pcp-PIA rules. Thus, we think that the graphite-like crystal structure probability of P2NAADD are low.

The CCS results of P2NNAAD show that there are not coplannar dimers observed in relatively low energy area. Thus, we think that the graphite-like crystal structure probability of P2NNAAD are low.

The CCS results of P3NAAD-5 show that the azide group in the only relatively planar dimer has a 31^{o} dihedral angle relative to the molecular parent ring, which actually breaks up the flatness of dimer. Thus, we think that the graphite-like crystal structure probability of P3NAAD-5 are low.

For P3NNAD-1, there are three coplanar dimers found through CCS calculations. However, these dimers is unlikely to form a molecular chain after a careful deduction.

Thus, the graphite-like crystal structure possibility of P3NNAD-1 could be also eliminated according to our CCS and pcp-PIA rules

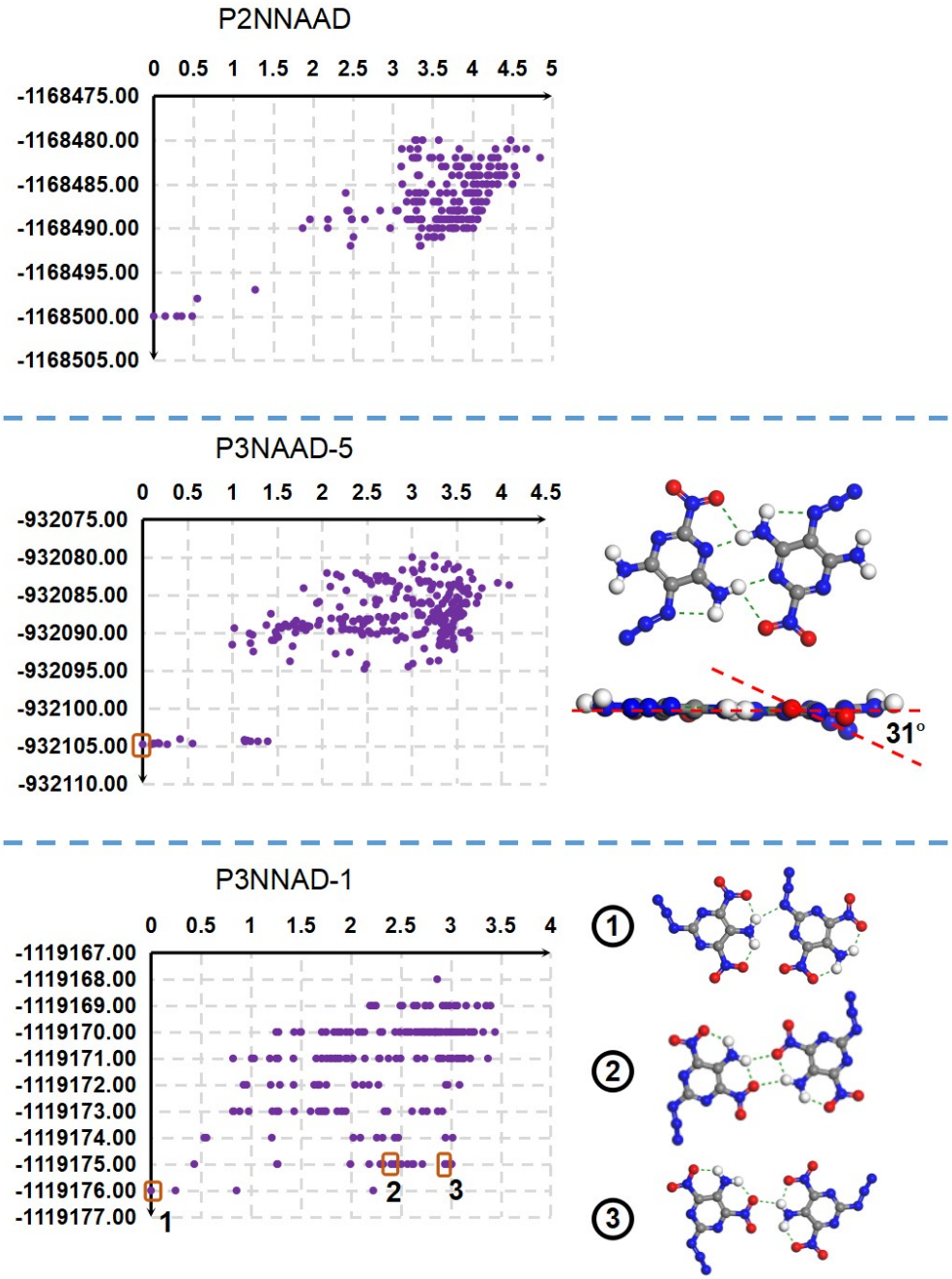

Figure S6. Sliding contour plots of DANAP, TATB and FOX-7

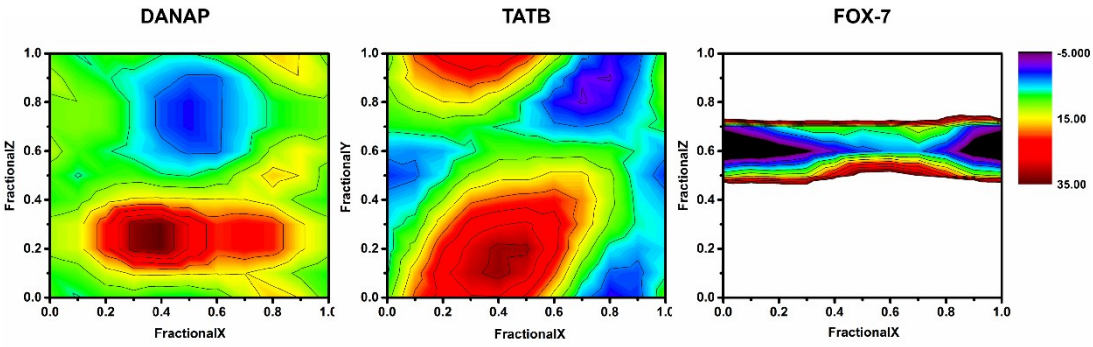

Sliding contour plots showing the total interaction energy versus the fractional coordinates of the centroid of the top layer of molecules for DANAP, TATB and FOX-7.

The interaction energy calculation are performed with Forcite module in Materials studio 8.0. The chosen forcefield is COMPASS.[2] The applicability of the COMPASS forcefield is validated through geometry optimization on the respective crystal structure.

The calculation procedure of detonation properties.

After acknowledging the density of DANAP, the solid state heat of formation must be calculated to obtain its detonation properties. The solid state heat of formation of DANAP can be calculated by below formula.

$$\Delta_{\mathrm{f}} H(\mathrm{solid},298k) = \Delta_{\mathrm{f}} H(\mathrm{g}as,298k) - \Delta_{\mathrm{sub}} H(298k)$$

The gas state heat of formation of DANAP (Δ_fH(gas)) that has direct correlation to the detonation properties of energetic material is calculated by G4(MP2)_6x method through Gaussian 09 (Revision D.01).[3,4] G4(MP2)_6x is a composite procedure with a lower cost but performance approaching that of G4. The new procedure employs BMK/6-31+G(2df,p) geometries and has six additional scaling factors for the correlation energy components.

The heat of sublimation (Δ_{sub}H) is estimated by the following equation. T is the meltpoint or decomposition point temperature in Kelvin.

$$\Delta_{\mathit{S}\mathrm{ub}} H = 0.188 \times T$$

Finally, the detonation velocity and detonation pressure can be estimated by Explo5 (version 6.02) software.

Table S1. Single crystal X-ray diffraction data of DANAP

Single crystal X-ray diffraction data was collected on an Oxford Xcalibur diffratometer with Mo-K_α monochromated radiation (λ=0.71073 Å). The crystal structures were solved by direct methods. The

structures were refined on F^2 by full-matrix least-squares methods using the SHELXTL script package.[5] All non-hydrogen atoms were refined anisotropoically.

CCDC	1960100
Formula	C4H4N8O2
Mr	196.15
Crystal system	orthorhombic
Space group	Pbca
a [Å]	7.040(4)
b [Å]	12.714(8)
c [Å]	16.640(10)
α [°]	90
β [°]	90
γ [°]	90
V [Å^3]	1489.4(15)
Z	8
T(K)	170
ρ[g cm^{-3}]	1.750
Mu [mm^{-1}]	0.145
F(000)	800
θ [°]	3.20 to 27.18
index range	$-8 \leq h \leq 9$
	$-16 \leq k \leq 6$
	$-21 \leq l \leq 21$
reflections collected	4540
independent reflections	1646[R_{int} = 0.0637, R_{sigma} = 0.0780]
data/restraints/parameters	1646/0/127
GOF on F^2	1.018
*R*1 [I>2σ(I)]	0.0830
*wR*2 [I>2σ(I)]	0.2098

*R*1(all data)	0.1409
*wR*2(all data)	0.2500
largest diff. peak and hole [e Å^{-3}]	0.785/-0.345

^{1}H,^{13}C NMR spectra of intermediates and DANAP

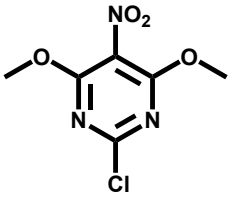

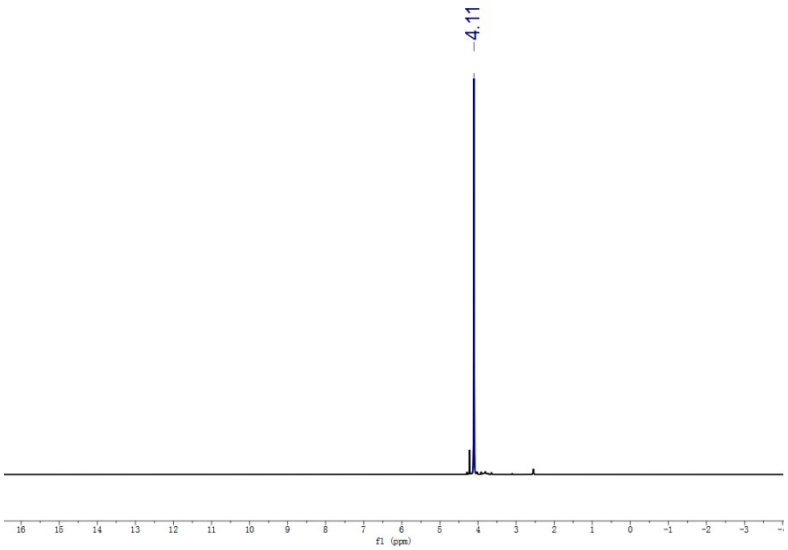

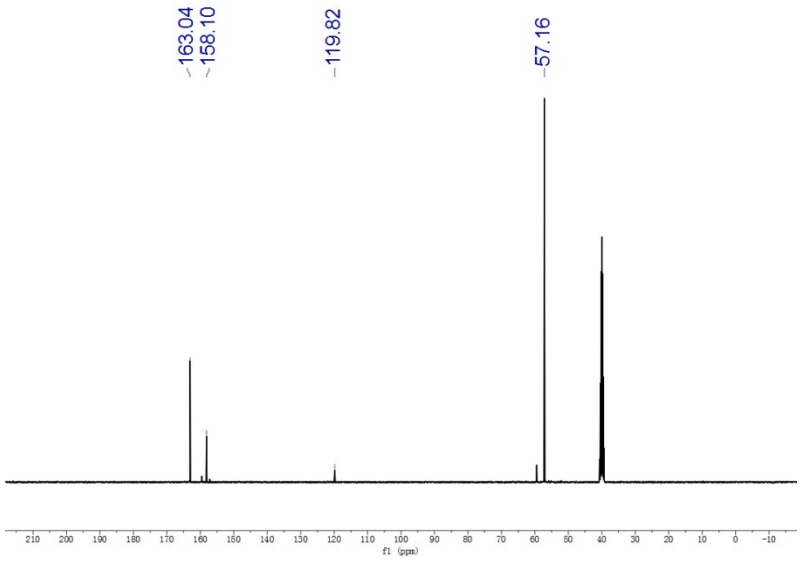
163.04
158.10
119.82
57.16
210 200 190 180 170 160 150 140 130 120 110 100 90 80 70 60 50 40 30 20 10 0 -10
f1 (ppm)

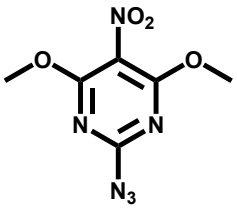
NO2
O
O
N
N
N3

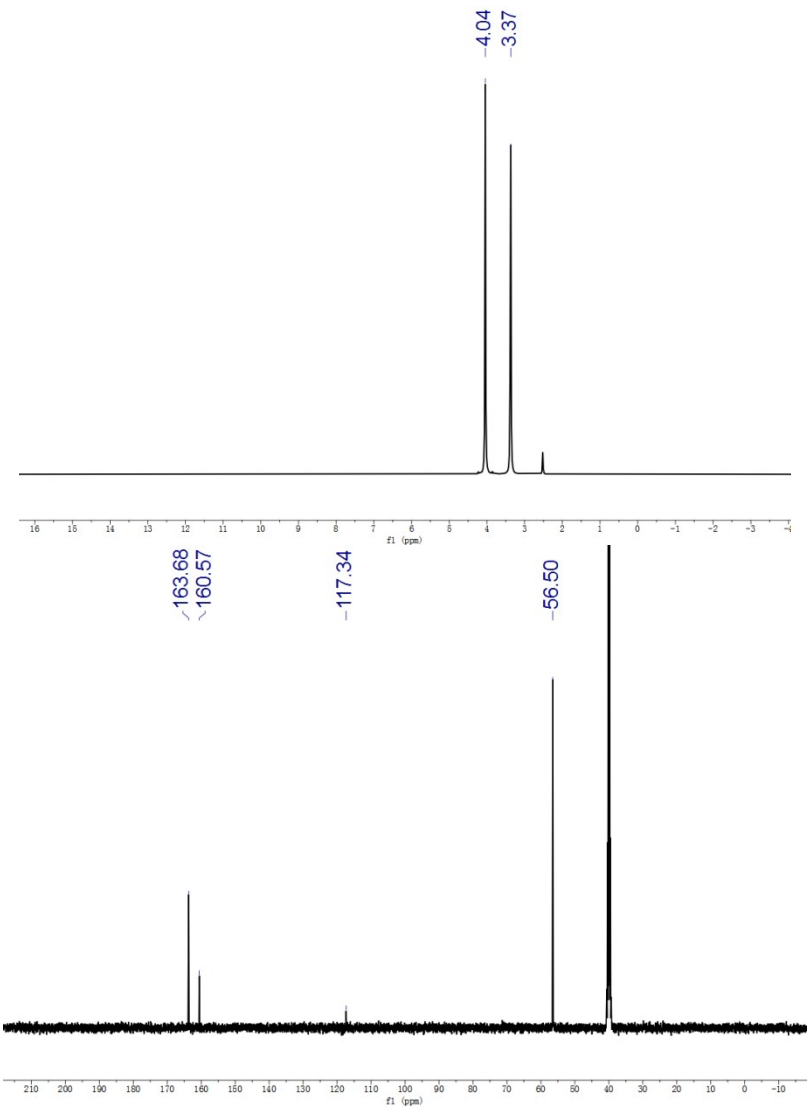
4.04
3.37
f1 (ppm)
163.68
160.57
117.34
56.50
f1 (ppm)

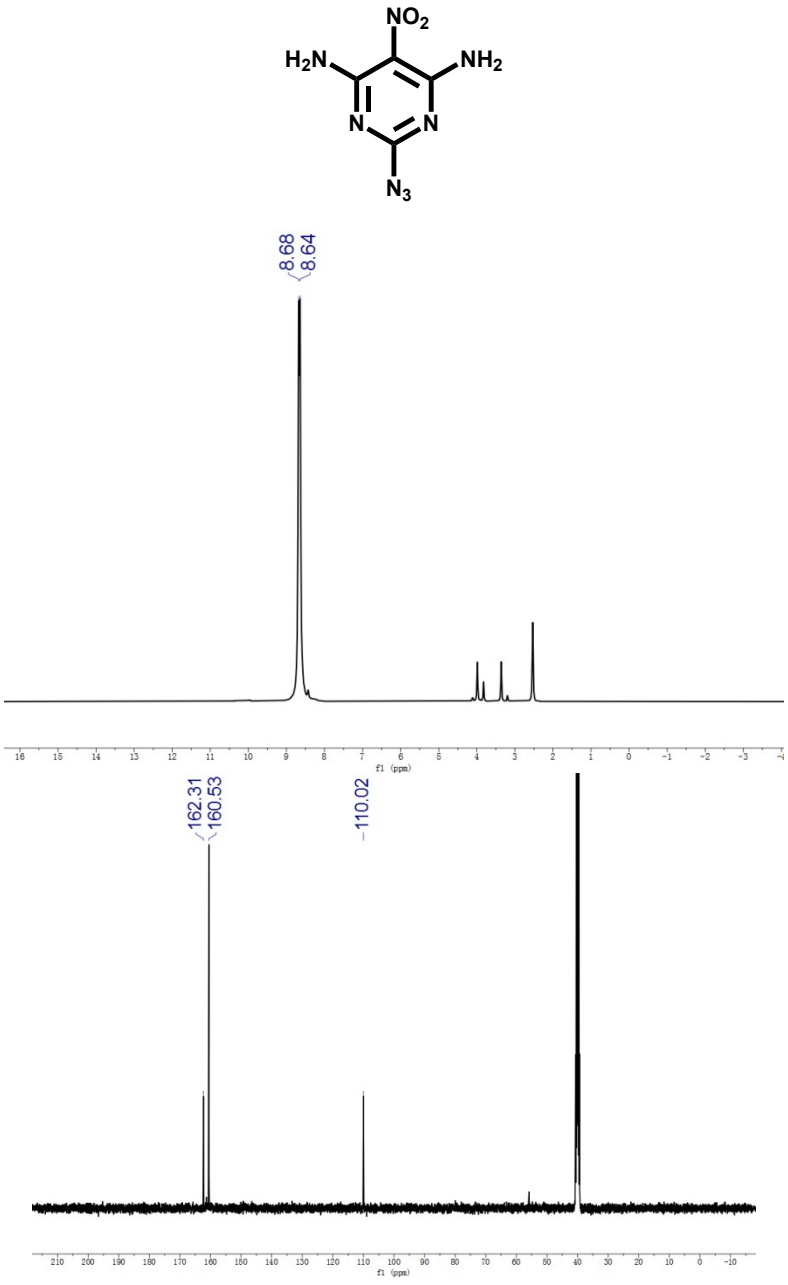
NO2
H2N
NH2
N
N
N3
8.68
8.64
f1 (ppm)
162.31
160.53
110.02
f1 (ppm)

References

[1] Grimme, S. Semiempirical GGA-Type Density Functional Constructed with a Long-Range Dispersion Correction. J. Comput. Chem. 2006, 27 (15), 1787-1799.
[2] Sun H. COMPASS: an ab initio force-field optimized for condensed-phase applications overview with details on alkane and benzene compounds. *J. Phys. Chem. B* **1998**, 102(38): 7338-7364.
[3] Chan, B.; Deng, J.; Radom, L. G4(MP2)-6X: A Cost-Effective Improvement to G4(MP2). *J. Chem. Theory Comput.* ***2011***, *7*, 112–120.
[4] Gaussian 09, Revision D.01, M. J. Frisch, G. W. Trucks, H. B. Schlegel, G. E. Scuseria, M. A. Robb, J. R. Cheeseman, G. Scalmani, V. Barone, B. Mennucci, G. A. Petersson, H. Nakatsuji, M. Caricato, X. Li, H. P. Hratchian, A. F. Izmaylov, J. Bloino, G. Zheng, J. L. Sonnenberg, M. Hada, M. Ehara, K. Toyota, R. Fukuda, J. Hasegawa, M. Ishida, T. Nakajima, Y. Honda, O. Kitao, H. Nakai, T. Vreven, J. A. Montgomery, Jr., J. E. Peralta, F. Ogliaro, M. Bearpark, J. J. Heyd, E. Brothers, K. N. Kudin, V. N. Staroverov, T. Keith, R. Kobayashi, J. Normand, K. Raghavachari, A. Rendell, J. C. Burant, S. S. Iyengar, J. Tomasi, M. Cossi, N. Rega, J. M. Millam, M. Klene, J. E. Knox, J. B. Cross, V. Bakken, C. Adamo, J. Jaramillo, R. Gomperts, R. E. Stratmann, O. Yazyev, A. J. Austin, R. Cammi, C. Pomelli, J. W. Ochterski, R. L. Martin, K. Morokuma, V. G. Zakrzewski, G. A. Voth, P. Salvador, J. J. Dannenberg, S. Dapprich, A. D. Daniels, O. Farkas, J. B. Foresman, J. V. Ortiz, J. Cioslowski, and D. J. Fox, Gaussian, Inc., Wallingford CT, 2013.
[5] Sheldrick, G. M. Crystal structure refinement with SHELXL. *Acta Crystallogr. Sec. C* **2015**, 71(1): 3-8.